Journal of Power Sources 232 (2013) 193–198

Contents lists available at SciVerse ScienceDirect

Journal of Power Sources

journal homepage: www.elsevier.com/locate/jpowsour

# Nanoporous anatase $TiO_2$/single-wall carbon nanohorns composite as superior anode for lithium ion batteries

Wei Xu [a], Zhiyong Wang [a], Zhengduo Guo [a], Yang Liu [a], Nengzhi Zhou [a], Ben Niu [a], Zujin Shi [a,*], Hao Zhang [b,**]

[a] Beijing National Laboratory for Molecular Sciences, State Key Lab of Rare Earth Materials Chemistry and Applications, College of Chemistry and Molecular Engineering, Peking University, Beijing 100871, China
[b] Research Institute of Chemical Defense, West Building, 35 Huayuanbei Road, Beijing 100083, China

## HIGHLIGHTS

- A novel composite of $TiO_2$/SWCNHs was facilely synthesized.
- The SWCNHs severed as a superior conducting network.
- The composite exhibits a promising anode material for lithium ion batteries.
- The composite can be achieved in low cost and large scale.

## GRAPHICAL ABSTRACT

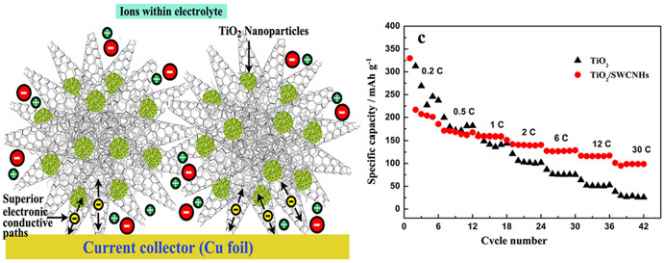


## ARTICLE INFO

*Article history:*
Received 9 June 2012
Received in revised form
12 December 2012
Accepted 15 December 2012
Available online 18 January 2013

*Keywords:*
Lithium ion battery
High rate capability
Anode
Composite

## ABSTRACT

A novel composite of single-wall carbon nanohorns (SWCNHs ) supported nanoporous anatase $TiO_2$, $TiO_2$/SWCNHs, is facilely synthesized by hydrolysis of tetrabutoxytitanium in the presence of SWCNHs. The phase structure, morphology, and pore structure of $TiO_2$/SWCNHs are investigated with transmission electron microscopy, X-ray diffraction and the nitrogen adsorption and desorption isotherms measurements. The $TiO_2$/SWCNHs composite materials show excellent electrochemical properties, and are expected to be a promising anode material for high power density lithium ion batteries. It is found that the $TiO_2$/SWCNHs composite not only exhibits excellent cycling performance, but also shows high rate capability as anode materials by the cyclic voltammetry and constant current discharge–charge tests. Especially, the specific charge capacity of the $TiO_2$/SWCNHs composite remains as high as 100 mAh $g^{-1}$ at a high rate of 30 C, which is four times higher than that of pure $TiO_2$ anode materials. The SWCNHs with high rate production in low cost have hopeful application to electrode materials for lithium ion batteries.


## 1. Introduction

Lithium ion batteries have been regarded as one of the most promising candidates for applications in electric and hybrid vehicles, if only their electric power storage and rate performances can be further improved [1–4]. In general, high performance lithium ion batteries require low weight, low volume, low cost and environmental benignity. To achieve this target, novel anode materials with rapid ion and electron transporting are badly needed, so recently anode materials the relevant researches have become one of the focus areas in lithium ion battery study [5,6].

Anode materials made of nanosized metal oxides have been intensively investigated since the pioneer work by Tarascon [3]. In our research, we have special interest in nanostructured $TiO_2$ as inspired by its different advantages when they are used as anode

* Corresponding author. Tel.: +86 10 62751495; fax: +86 10 62751708.
** Corresponding author. Tel.: +86 10 66705840; fax: +86 10 66748499.
*E-mail addresses:* zjshi@pku.edu.cn (Z. Shi), dr.h.zhang@hotmail.com (H. Zhang).

0378-7753/$ – see front matter © 2013 Elsevier B.V. All rights reserved.
http://dx.doi.org/10.1016/j.jpowsour.2012.12.115

materials in lithium ion batteries. The excellent volumetric and gravimetric storage capacities [7–9], as well as high stability and safety during lithium ion batteries cycling, make $TiO_2$ a promising anode material in the future lithium ion batteries. Most importantly, we demonstrate a high packing density here is achieved by mesoporous $TiO_2$. This novel mesoporous $TiO_2$ would be a superior material for Lithium ion batteries with high rate capabilities. However, to make practical application of $TiO_2$ for lithium ion batteries, it has still a challenge to overcome the low lithium diffusivity inside $TiO_2$, which would determine the lithium insertion and extraction rates [10].

To improve the performance of $TiO_2$ anode, various metals, metal oxides and carbonaceous materials, e.g., $TiO_2$/Ag [11], $TiO_2$/Cu (or Sn) [12,13], $TiO_2$/$RuO_2$ [14], $TiO_2$/carbon nanotubes [15,16] and $TiO_2$/graphene [1] nanocomposites etc., have been utilized as matrices or conductive additives to improve the conductivity and electrochemical performance for lithium storage. Among them, carbon nanomaterials have attracted special attention due to their large specific surface area, strong corrosion resistance and low price. For example, single-wall carbon nanotubes (SWCNTs) not only own high electronic conductivity, but also have excellent Li-storage ability at a low voltage making it as attractive anode material in lithium ion batteries [17]. The incorporation of SWCNTs inside or beside a mesoporous anatase $TiO_2$ phase by means of the bicontinuous microemulsion-aided process effectively improves the charging–discharging property of anatase $TiO_2$, especially at high rate. However, the cost of their synthesis is viable remains an open question. To become commercially viable, a cost effective coating material is desired to replace the expensive SWCNTs.

SWCNHs are new carbon nanomaterials that are composed of single layer graphene similar to SWCNTs. SWCNHs could be produced by laser ablation or direct current (DC) arc-discharge vaporization of pure graphite without the use of expensive metal catalysts under air atmosphere, thereby making them more cost-effective than SWCNTs [18]. Recently, low cost and large scale of production of SWCNHs were achieved by arc evaporation of a graphite rod in air atmosphere in our group [19]. Moreover, SWCNHs were found to have many superior features such as large specific surface areas, variable porosity, and high electrical conductivity etc., so they are believed to be excellent candidates for anode materials of lithium ion batteries. Zhao et al. recently reported SWCNHs coated $Fe_2O_3$ anode materials that showed high rate performance and cycling stability [20], confirming above prediction preliminarily. In this paper, we further show the synthesis of a novel composite of SWCNHs supported nanoporous anatase $TiO_2$/SWCNHs. Furthermore, we also demonstrate that the capacity at high charging–discharging rates increases for SWCNHs containing nanoporous $TiO_2$ compared with that of pure nanoporous $TiO_2$. In the composite of $TiO_2$/SWCNHs, the SWCNHs assist the storage in $TiO_2$ by providing electrons, and the capacity of $TiO_2$/SWCNHs at a high rate (100 mAh $g^{-1}$ at 30 C) was higher than that of the reported $TiO_2$/SWCNTs (85 mAh $g^{-1}$ at 30 C) [17]. More importantly the composite we prepared in the report can be produced in a large scale.

## 2. Experimental

### 2.1. Preparation of $TiO_2$/SWCNHs and $TiO_2$ nanoporous structures

The synthesis of anatase $TiO_2$/SWCNHs composite is achieved by controlled hydrolysis of tetrabutoxytitanium in the presence of SWCNHs. Briefly, SWCNHs was synthesized by an arc discharge

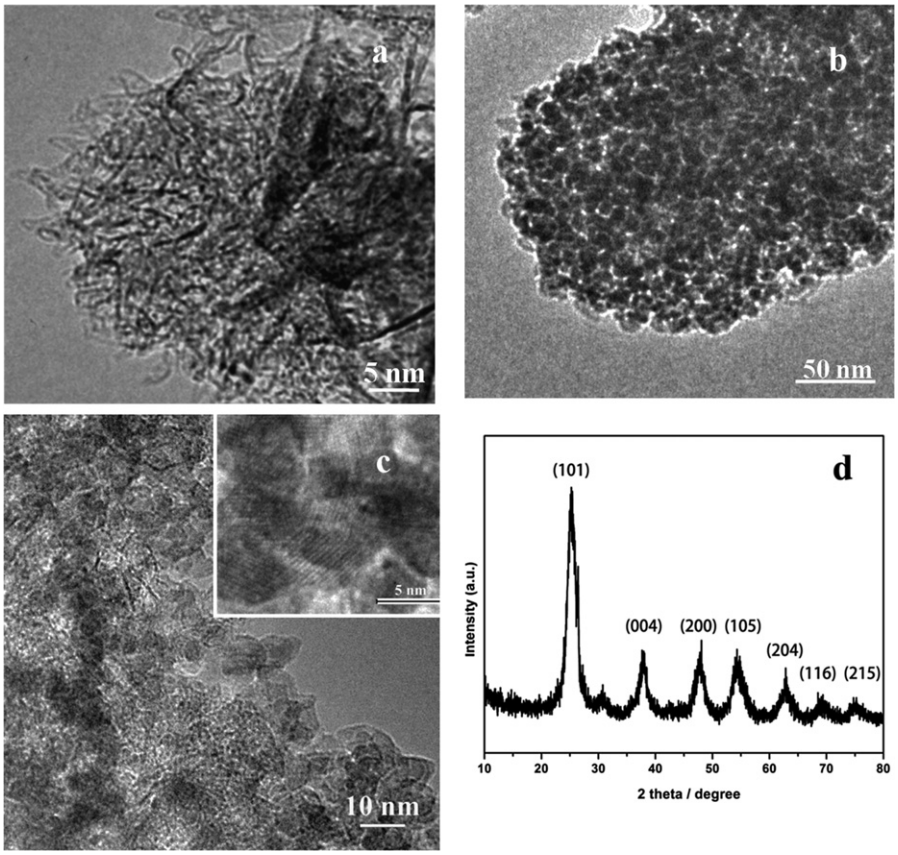


**Fig. 1.** (a) TEM image of SWCNHs. (b) TEM image of a $TiO_2$/SWCNHs composite. (c) HRTEM images of $TiO_2$/SWCNHs composite. (d) XRD pattern of $TiO_2$/SWCNHs composite.

method as described in our previous report [19], and all the reagents were used as received with analytical grade purity. In a typical process, the SWCNHs were annealed in air for 40 min at 400 °C to remove amorphous carbon impurity and open the nanohorns, which would increase the surface area of SWCNHs and make them more dispersible in organic solvents [21], and then 30 mg of the SWCNHs were ultrasonically dispersed in 50 mL of ethylene glycol for 5 h. Afterwards, 600 μL tetrabutoxytitanium (Beijing Chemicals Co.) was added and was magnetically stirred for 8 h at room temperature, and the mixture was poured into a solution mixture with 170 mL acetone (Beijing Chemicals Co.) and 2.7 mL water. After vigorous stirred for one more hour, the precipitate was harvested by centrifugation, followed by washing with ethanol for five times and was dried at 50 °C for further usage. Finally, the as-prepared $TiO_2$-precursor coated SWCNHs were added to 20 mL water and were heated to reflux under stirring. After refluxing about an hour, the precipitate was obtained by centrifugation, followed by washing with water five times and was dried at 50 °C to obtain crystalline $TiO_2$/SWCNHs composites.

For comparison, the nanoporous $TiO_2$ was prepared by a similar process but without SWCNHs added according to the literature [22]. In a typical procedure, 2 mL tetrabutoxytitanium was added to 50 mL ethylene glycol and was magnetically stirred for 8 h at room temperature, then the mixture was poured into a solution containing 170 mL acetone and 2.7 mL water, and was vigorous stirred for an hour. The titanium glycolate precursor was harvested by centrifugation, followed by washing with ethanol for five times and was dried at 50 °C. 0.1 g $TiO_2$-precursor was added to 20 mL water and was heated to reflux under stirring. After refluxing for an hour, the white $TiO_2$ nanoparticals was obtained by centrifugation followed by washing with water for five times and was dried at 50 °C for further usage.

### 2.2. Structure and morphology characterization

The morphologies and structures of the as-prepared samples were characterized by scanning electron microscopy (SEM, JEOL 6701F) and transmission electron microscopy (TEM, Hitachi H-9000NAR). The X-ray diffraction (XRD) patterns were measured by a Rigaku D/max-2000 using filtered Cu Kα radiation. Pore size distributions of the samples were obtained from analysis of the nitrogen adsorption and desorption isotherms at 77.3 K with a Nova 2000e Surface Area-Pore Size Analyzer. Thermogravimetric analysis (TGA) was carried out using a Q600 TGA analyzer (Thermal Analysis Inc.) from room temperature to 900 °C at a ramp rate of 10 °C $min^{-1}$ under an air flow of 100 mL $min^{-1}$.

### 2.3. Electrochemical characterization

Cyclic voltammetry measurements were carried out by using three-electrode cells with lithium metal as the counter and reference electrodes. Galvanostatic measurements were carried out by using two-electrode cells with lithium metal as the counter electrode. The working electrodes were fabricated by compressing the mixture of 90 wt% nanoporous $TiO_2$ or $TiO_2$/SWCNHs composites and 10 wt% polytetrafluoroethylene onto a copper foil. The working electrodes were dried in vacuum at 120 °C for at least 4 h and then assembled as cells in an Ar-filled glovebox (MBRAUN, UNIlab,

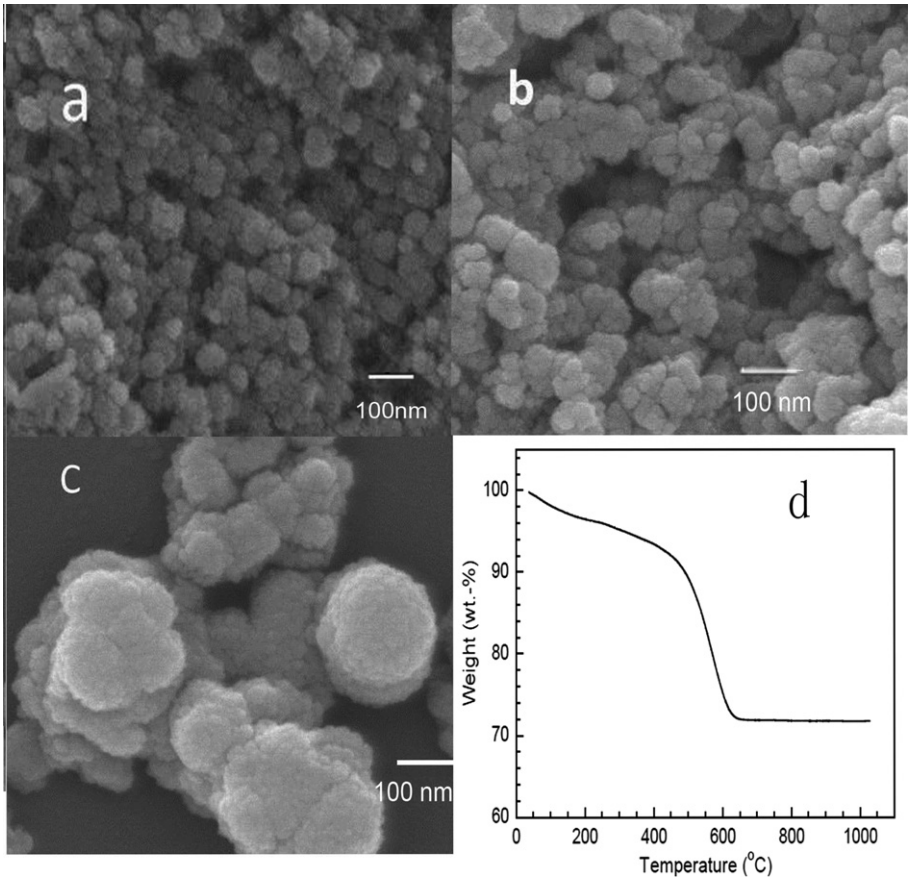


**Fig. 2.** a) Typical SEM images of SWCNHs used in the experiments. b) Typical SEM images of $TiO_2$/SWCNH. c) Typical SEM images of $TiO_2$ sample synthesized under the control experiment in the absence of SWCNHs. d) Thermogravimetry curves of $TiO_2$/SWCNHs composite from 30 to 900 °C under flowing air.

Germany). The electrolyte used was 1.0 mol $L^{-1}$ $LiPF_6$ in a 50:50 (*v*/*v*) mixture of ethylene carbonate and dimethyl carbonate. Cyclic voltammograms were recorded from 2.5 to 1.0 V at 0.5 mV $s^{-1}$, by using a Solartron 1280Z electrochemical workstation. The charge–discharge measurements were carried out using an Arbin BT-2000 system. Galvanostatic cycling was performed between 2.5 and 1.0 V at various rates to evaluate the rate and cycle performance. All measurements were carried out at room temperature.

## 3. Results and discussion

TEM images of the SWCNHs aggregates before and after anatase titanium oxide deposition are presented in Fig. 1, respectively. Fig. 1a shows typical 'dahlia-like' morphology of SWCNHs where the nanohorns protrude from the aggregate surface. The pure mesoporous $TiO_2$ sphere was shown in Fig. 1b. After hydrolysis of tetrabutoxytitanium in the presence of SWCNHs, $TiO_2$ nanoparticles had been self-assembled and well attached on the sphere aggregate of SWCNHs. Even after ultrasonication in ethanol for 30 min for TEM observation, $TiO_2$ particles are still well attached on SWCNHs, as shown in Fig. 1c. A high-resolution TEM image reveals that the $TiO_2$ particles are well crystallized, and the particle size is about 3–5 nm. The nanocrystal is assigned to anatase phase of $TiO_2$ (JCPDS No. 21-1272) based on XRD analysis (Fig. 1d) except for a small diffraction peak at about 30.8°, corresponding to brookite $TiO_2$ (JCPDS Card No. 29-1360). The HRTEM image also reveals the high porous structure of the $TiO_2$/SWCNHs composite. The magnified SEM images (see Fig. 2) disclose the rough surface of the $TiO_2$/SWCNHs composite.

TGA was used to determine the chemical composition of the final composites. The result shows that the composites have a chemical composition of 72 wt % of $TiO_2$ and 28 wt % of SWCNHs (Fig. 2d).

To further investigate the pore structure of the samples, nitrogen isothermal adsorption/desorption technique was used. Fig. 3 shows the adsorption/desorption isotherms that exhibit a hysteresis typical of a porous system. According to Brunauer–Emmett–Teller (BET) analysis, a total specific surface area of 264 $m^2$ $g^{-1}$ and 195 $m^2$ $g^{-1}$ are obtained for $TiO_2$ and $TiO_2$/SWCNHs composites, respectively, which are significantly higher than that of most reported porous titania [16,23,24]. The relative large specific surface area would be beneficial for electrolyte access. Although the incorporation of SWCNHs into the $TiO_2$ system results in a decrease in BET surface area, Fig. 3 shows that the pore size of $TiO_2$/SWCNHs composite was increased comparing with that of $TiO_2$. It is expected that the porous materials with large pore sizes would be much better for a smooth transport of electrolyte ions.

For high power lithium ion batteries, it is always desirable to have excellent high-rate performance [25]. However, $TiO_2$ anode materials behave poor power density at high charging–discharging rates [7,23,25,26]. It was revealed that the materials show slow lithium diffusion in the solid active material that increases the resistances both of the active materials and electrolyte. Therefore, a good way to resolve this problem is to design and fabricate nanostructured electrode materials that provide interconnected nanopaths for electrolyte-ion transport and electronic conduction. In this sense, it is not strange to observe the better performance of SWCNHs fabricated $TiO_2$ composites than that of $TiO_2$ anode in lithium ion batteries especially at high discharge–charge rates.

In order to demonstrate the potential application of the $TiO_2$/SWCNHs composite in improving rate-capacity for anode materials of lithium ion batteries, Lithium-ion insertion/extraction properties of the $TiO_2$/SWCNHs composite and the bare $TiO_2$ anode have been investigated by cyclic voltammetry and galvanostatic charging–discharging measurements, and the electrochemical performances

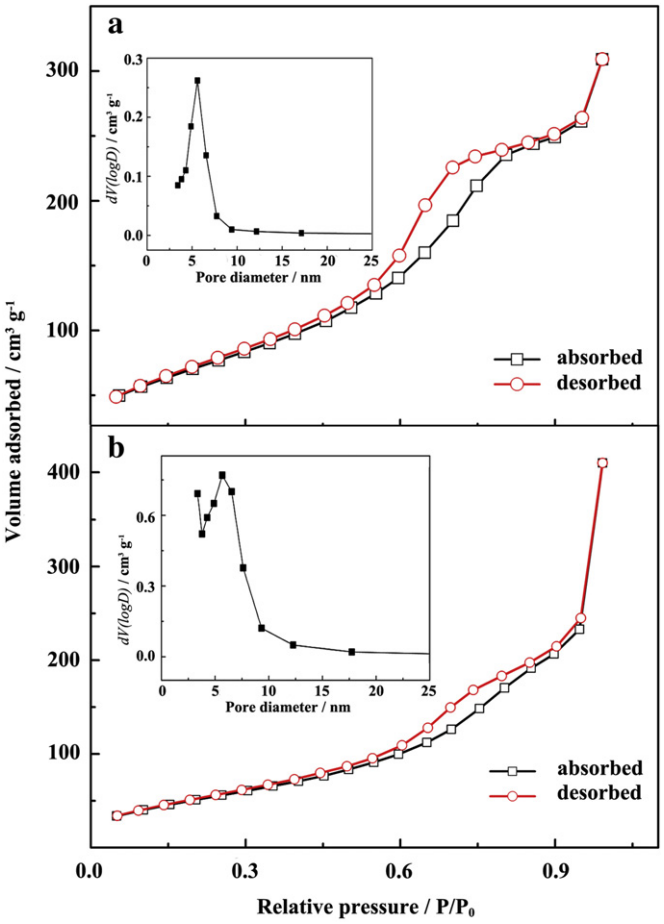


**Fig. 3.** $N_2$ adsorption–desorption isotherms of $TiO_2$ (curve a) and $TiO_2$/SWCNHs composite (curve b). The insets show BJH pore-size distributions of these samples.

of the samples were compared. Fig. 4a displays the typical discharge and charge curves of $TiO_2$/SWCNHs and bare $TiO_2$ electrode at a rate of 0.2 C (1 C corresponds to 150 mA $g^{-1}$). The typical discharge and charge capacities for $TiO_2$ are 227 and 196 mAh $g^{-1}$, respectively, and the Coulombic efficiency is 86.3%. In comparison, the $TiO_2$/SWCNHs composite owns typical discharge and charge capacities at 207 and 183 mAh $g^{-1}$(the capacity of the $TiO_2$/SCWCNHs composite was calculated based on the whole mass), respectively, with a relative higher Coulombic efficiency of 88.4%. Generally, increasing the specific surface area induces a substantial capacitive contribution to the overall capacity. Benefiting from their higher specific surface areas, the bare mesoporous $TiO_2$ electrode and the composite one both show relative high charge/discharge capacities [27–29]. Particles with higher surface area tend to result in an electrode with higher electrode/electrolyte contact area, which, in turn, leads to facilitate $Li^+$ transport due to the shortened diffusion paths and the high specific capability. Meanwhile, the relative higher Coulombic efficiency of the $TiO_2$/SWCNHs composite electrode can be attributed to SWCNHs. The SWCNHs with high conductivity can form a good conductive network for the embedded active material of $TiO_2$. In this way the polarization during the lithium insertion/extraction process can be depressed [15]. The result demonstrates that the incorporation of SWCNHs in the $TiO_2$ makes the electrode more stable and reversible. The CV measurement was carried out (scan rate: 0.5 mV $s^{-1}$), and the result is presented in Fig. 4b. In the controlled potential scan, the electrode was cycled over a voltage window of 1.0–2.5 V. The CVs of the sample exhibited a pair of cathodic/anodic peaks at 1.70/2.06 V for $TiO_2$/SWCNHs composite

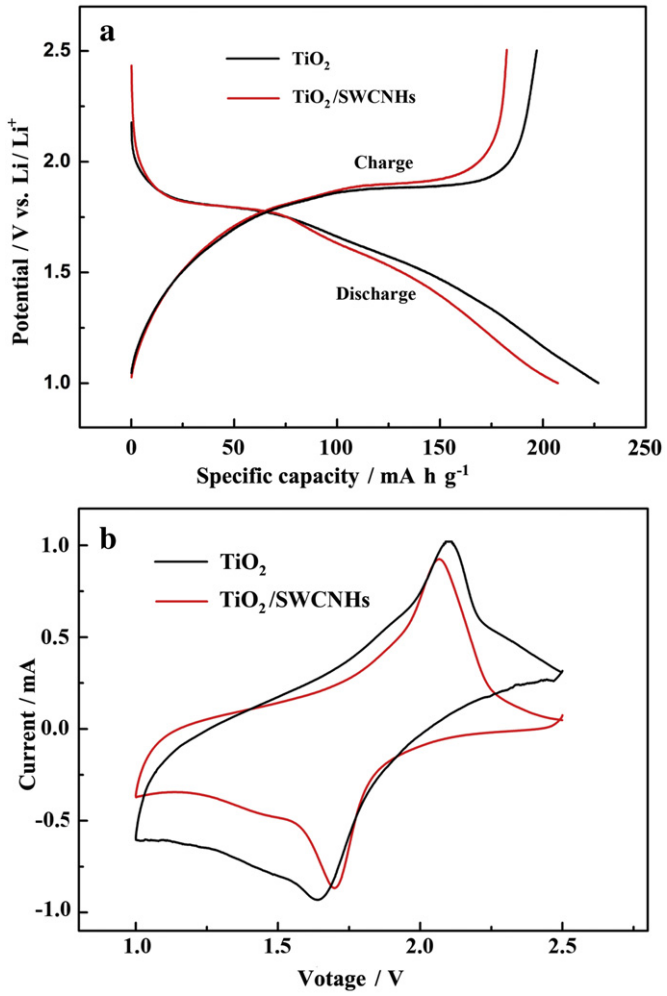


**Fig. 4.** (a) The discharge and charge curves of $TiO_2$/SWCNHs (red) and $TiO_2$ (dark) at a current density of 0.2 C in the third cycle. (b) Cyclic voltammogram of $TiO_2$/SWCNHs (red) and $TiO_2$ (dark) electrode at a scan rate of 0.5 mV $s^{-1}$. (For interpretation of the references to color in this figure legend, the reader is referred to the web version of this article.)

and 1.64/2.10 V for bare $TiO_2$, which are characteristic for the lithium-ion insertion/extraction in anatase $TiO_2$, since the Li storage in carbon materials is mainly occurring below 1 V, and the reversible Li storage in $TiO_2$ is usually reported between 1 and 3 V [30–32]. The cathodic (insertion) and anodic (extraction) peaks are in accordance with the plateaus of the discharging/charging curves. Both of them show much greater reversible Li storage. The reversible Li storage in the nanoporous anatase $TiO_2$ of $TiO_2$/SWCNHs is much better than that of bare anatase $TiO_2$. The much lower polarization value of $TiO_2$/SWCNHs composite electrode (0.36 V) than that of the bare $TiO_2$ electrode (0.46 V) indicate that the lithium intercalation/extraction reaction proceeds much easier for the $TiO_2$/SWCNHs composite [33,34]. These results demonstrate improved kinetics for $Li^+$ insertion/extraction in the $TiO_2$/SWCNHs composite electrode structures attributed to the good electronic conductivity of SWCNHs. Thereby, SWCNH is also a fine Li-storage host as well as a fast Li insertion-extraction host at a low voltage, which makes it an attractive matrix of anode material for lithium-ion batteries [17].

To investigate the rate performance of the $TiO_2$/SWCNHs composites, the lithium ion batteries were cycled at various rates. The charge–discharge capacity of $TiO_2$ decreased steeply along with the current density increasing (Fig. 5a). On the other hand, the capacity of the $TiO_2$/SWCNHs composites shows relatively small decrease with the current density increasing (Fig. 5b), indicating a better power performance of the lithium ion batteries by this composite material, especially at high C rates.

Fig. 5c shows the rate performances of lithium ion batteries by the $TiO_2$/SWCNHs composite and the bare $TiO_2$. At a low C rates (<1C), $TiO_2$ shows a higher discharge capacity than $TiO_2$/SCWNHs composite. It's reasonable considering the fact that the larger surface area of $TiO_2$ can lead to a shorter diffusion length of $Li^+$ in the solid phase;

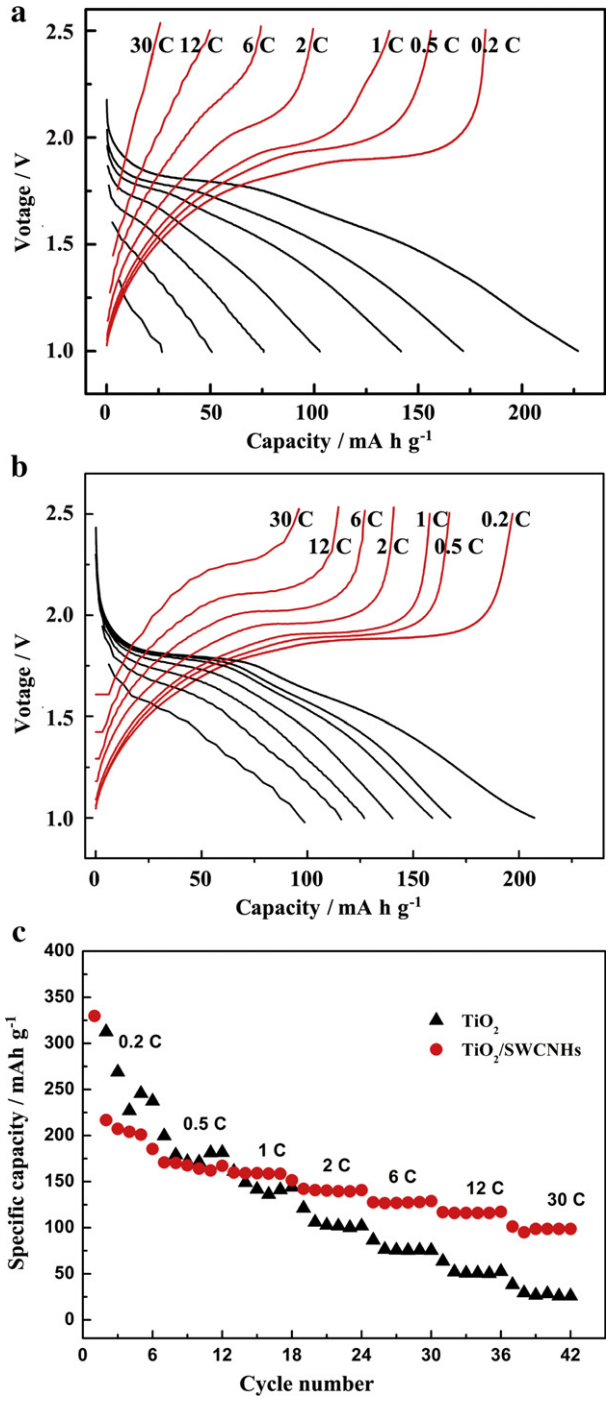


**Fig. 5.** The discharge and charge curves of $TiO_2$ (a) and $TiO_2$/SWCNHs (b) at various current densities from 0.2 C to 30 C in the third cycle. (c) Cycling performance of $TiO_2$/SWCNHs composite (red) and bare $TiO_2$ (dark) at various charge–discharge rates. All of the measurements were conducted using a voltage window of 1.0–2.5 V. (For interpretation of the references to color in this figure legend, the reader is referred to the web version of this article.)

meanwhile, a larger electrode/electrolyte contact can be expected [27,28]. In addition, the capacity of the $TiO_2$/SCWCNHs composite was calculated based on the whole mass, this may also lead to the reason of the lower of capacity. Upon increasing the C rate, the capacity of $TiO_2$ decreased steeply and it turns to be 25 mAh $g^{-1}$ at 30 C. On the contrary, the capacity of the $TiO_2$/SWCNHs composite will fade in a much slower way when the current is increased. Its discharge capacity can still retain a value above 100 mAh $g^{-1}$ at 30 C, which is four times higher than that of the reference $TiO_2$. This improved performance observed on the $TiO_2$/SWCNHs composite suggested that electron-conducting paths play an important role during the charge/discharge at high C. With the help of SWCNHs, the polarization at high C rates can be successfully alleviated due to the improved conductivity of the electrode, resulting in a higher discharge capacity for this $TiO_2$/SWCNHs composite.

Based on the above results and analyses, the improved energy storage features of the $TiO_2$/SWCNHs composite at high C rates are illustrated in Fig. 6, i.e., the fabricated nanostructured $TiO_2$/SWCNHs composite electrode materials provided interconnected nanopaths for electrolyte-ion transport and electronic conduction.

In summary, the composite electrode materials have several advantages. First, SWCNHs possess good electrical conductivity, which severed as superior conducting network allows for efficient charge transport and enhances the electronic conductivity of composite significantly. Second, the high surface area and the large mesopore size reduce the diffusion length of ions within $TiO_2$ phase during the charge/discharge process [35], leading to a stable cycle performance of $TiO_2$/SWCNHs composite at high rates. Third, the special structural features of mesoporous composite electrodes enhance the ionic conductivity greatly, and ion-buffering reservoirs can be formed in these mesopores to minimize the diffusion distances to interior surfaces of $TiO_2$ [36]. Fourth, SWCNHs own exceptional mechanical properties, so SWCNHs supported $TiO_2$ nanoparticles can release the cycle degradation caused by the mechanical stresses or volume changes, thus overcome $TiO_2$ nanoparticle aggregation [37]. In addition, every $TiO_2$ particle connects to the conducting framework directly, so some extra contacting resistance or weight increase from the binders or conducting additives are eliminated. Undoubtedly, $TiO_2$/SWCNHs composite is superior anode material for lithium ion batteries and may be widely applied in near future.

## 4. Conclusions

We successfully synthesized a novel $TiO_2$/SWCNHs composite with a simple wet chemistry method. As an anode material for lithium ion batteries, the $TiO_2$/SWCNHs composite exhibits superior electrochemical performance with high capacity and good rate performance, highlighting the importance of the intimate interaction between SWCNHs substrate and $TiO_2$ nanoparticles. This $TiO_2$/SWCNHs composite delivers a high capacity of 100 mAh $g^{-1}$ even at a C rate of 30 C, which makes it a promising anode material for lithium ion batteries. More remarkably, the SWCNHs of used in composite $TiO_2$/SWCNHs can be produced in low-cost and large-scale and it may also be extended to other electrode materials for future electrochemical energy storage device.

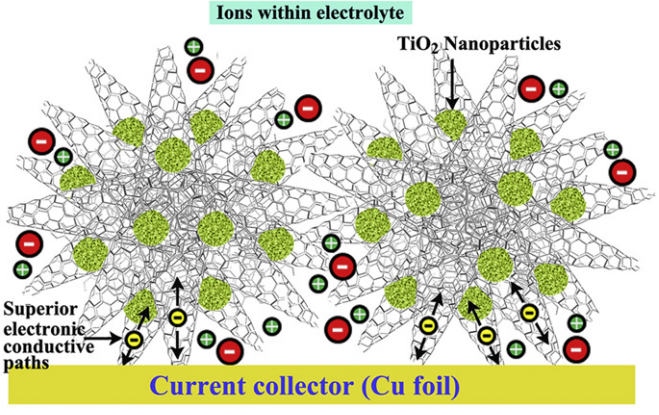


**Fig. 6.** Schematic representation of the microstructure and energy storage characteristics of the $TiO_2$/SWCNHs composite.

## Acknowledgements

The authors gratefully acknowledge the Ministry of Science and Technology of China (No. 2013CB933402, 2011CB932601) for financial support and the National Natural Science Foundation of China (No. 21171013).

## References

[1] S. Yang, X. Feng, K. Müllen, Adv. Mater. 23 (2011) 3575–3579.
[2] P.G. Bruce, B. Scrosati, J.M. Tarascon, Angew. Chem. Int. Ed. 47 (2008) 2930–2946.
[3] M. Armand, J.M. Tarascon, Nature 451 (2008) 652–657.
[4] G.H. Kim, K. Smith, J. Ireland, A. Pesaran, J. Power Sources 210 (2012) 243–253.
[5] M.H. Park, K. Kim, J. Kim, J. Cho, Adv. Mater. 22 (2010) 415–418.
[6] Y.S. Hu, Y.G. Guo, W. Sigle, S. Hore, P. Balaya, J. Maier, Nat. Mater. 5 (2006) 713–717.
[7] S.T. Myung, N. Takahashi, S. Komaba, C.S. Yoon, Y.K. Sun, K. Amine, H. Yashiro, Adv. Funct. Mater. 21 (2011) 3231–3241.
[8] K. Saravanan, K. Ananthanarayanan, P. Balaya, Energy Environ. Sci. 3 (2010) 939–948.
[9] L.D. Noailles, C.S. Johnson, J.T. Vanghey, M.M. Thackeray, J. Power Sources 81/82 (1999) 259–263.
[10] J.Y. Shin, D. Samuelis, J. Maier, Adv. Funct. Mater. 21 (2011) 3464–3472.
[11] S.H. Nam, H.S. Shim, Y.S. Kim, M.A. Dar, J.G. Kim, W.B. Kim, ACS Appl. Mater. Interfaces 2 (2010) 2046–2052.
[12] M. Mancini, P. Kubiak, J. Geserick, R. Marassi, N. Hüsing, M. Wohlfahrt-Mehrens, J. Power Sources 189 (2009) 585–589.
[13] M. Mancini, P. Kubiak, M. Wohlfahrt-Mehrens, R. Marassi, J. Electrochem. Soc. 157 (2) (2010) A164–A170.
[14] Y.G. Guo, Y.S. Hu, W. Sigle, J. Maier, Adv. Mater. 19 (2007) 2087–2091.
[15] F.F. Cao, Y.G. Guo, S.F. Zheng, X.L. Wu, L.Y. Jiang, R.R. Bi, L.J. Wan, J. Maier, Chem. Mater. 22 (2010) 1908–1914.
[16] I. Moriguchi, R. Hidaka, H. Yamada, T. Kudo, H. Murakami, N. Nakashima, Adv. Mater. 18 (2006) 69–73.
[17] A. Odani, A. Nimberger, B. Markovsky, E. Sominski, E. Levi, V.G. Kumar, A. Motiei, A. Gedanken, P. Dan, D. Aurbach, in: 11th International Meeting on Lithium Batteries, Monterey, CA, June 22–28, 2002, Elsevier Science BV, Amsterdam, 2002, pp. 517–521.
[18] T. Yamaguchi, S. Bandow, S. Iijima, Chem. Phys. Lett. 389 (2004) 181–185.
[19] N. Li, Z. Wang, K. Zhao, Z. Shi, Z. Gu, S. Xu, Carbon 48 (2010) 1580–1585.
[20] Y. Zhao, J. Li, Y. Ding, L. Guan, Chem. Commun. 47 (2011) 7416–7418.
[21] H. Song, X. Qiu, F. Li, W. Zhu, L. Chen, Nano Res. 4 (2011) 290–296.
[22] L.S. Zhong, J.S. Hu, L.J. Wan, W.G. Song, Chem. Commun. 10 (2008) 1184–1186.
[23] S. Ding, J.S. Chen, Z. Wang, Y.L. Cheah, S. Madhavi, X. Hu, X.W. Lou, J. Mater. Chem. 21 (2011) 1677–1680.
[24] J.S. Chen, Y.L. Tan, C.M. Li, Y.L. Cheah, D. Luan, S. Madhavi, F.Y.C. Boey, L.A. Archer, X.W. Lou, J. Am. Chem. Soc. 132 (2010) 6124–6130.
[25] N. Li, G. Liu, C. Zhen, F. Li, L. Zhang, H.M. Cheng, Adv. Funct. Mater. 21 (2011) 1717–1722.
[26] H. Liu, Z. Bi, X.G. Sun, R.R. Unocic, M.P. Paranthaman, S. Dai, G.M. Brown, Adv. Mater. 23 (2011) 3450–3454.
[27] G. Sudant, E. Baudrin, D. Larcher, J.-M. Tarascon, J. Mater. Chem. 15 (2005) 1263–1269.
[28] Y.G. Guo, Y.S. Hu, J. Maier, Chem. Commun. (2006) 2783–2785.
[29] F.F. Cao, X.L. Wu, S. Xin, Y.G. Guo, L.J. Wan, J. Phys. Chem. C 114 (2010) 10308–10313.
[30] K.H. Reiman, K.M. Brace, T.J. Gordon-Smith, I. Nandhakumar, G.S. Attard, J.R. Owen, Electrochem. Commun. 8 (2006) 517–522.
[31] A.R. Armstrong, G. Armstrong, J. Canales, R. Garcia, P.G. Bruce, Adv. Mater. 17 (2005) 862–865.
[32] K.X. Wang, M.D. Wei, M.A. Morris, H.S. Zhou, J.D. Holmes, Adv. Mater. 19 (2007) 3016–3020.
[33] H. Lindström, S. Södergren, A. Solbrand, H. Rensmo, J. Hjelm, A. Hagfeldt, S.E. Lindquist, J. Phys. Chem. B 101 (1997) 7717–7722.
[34] P. Krtil, D. Fattakhova, L. Kavan, S. Burnside, M. Grätzel, Solid State Ionics 135 (2000) 101–106.
[35] Y.G. Wang, H.Q. Li, Y.Y. Xia, Adv. Mater. 18 (2006) 2619–2623.
[36] D.R. Rolison, Science 299 (2003) 1698–1701.
[37] C.K. Chan, H. Peng, G. Liu, K. McIlwrath, X.F. Zhang, R.A. Huggins, Y. Cui, Nat. Nano. 3 (2008) 31–35.